Foam Composites

Deutsche Ausgabe: DOI: 10.1002/ange.201600891
Internationale Ausgabe: DOI: 10.1002/anie.201600891

An Elastic Monolithic Catalyst: A Microporous Metalloporphyrin-Containing Framework-Wrapped Melamine Foam for Process-Intensified Acyl Transfer

Keyi Wu, Jia Guo, and Changchun Wang*

Abstract: *The advent of conjugated microporous polymers (CMPs) has had significant impact in catalysis. However, the presence of only micropores in these polymers often imposes diffusion limitations, which has resulted in the low utilization of CMPs in catalytic reactions. Herein, the preparation of a foam-supporting CMP composite with interconnective micropores and macropores and elastic properties is reported. Metalloporphyrin-based CMP organogels are synthesized within the melamine foam by a room-temperature oxidative homocoupling reaction of terminal alkynes. Upon drying, the CMP-based xerogels tightly wrap the framework skeletons of the foam, while the foam cells are still open to allow for the preservation of elasticity and macroporosity. Such a hierarchical structure is efficient for acyl transfer, facilitates substrate diffusion within interpenetrative macropores and micropores, and could be used to intensify catalytic processes.*

The two main routes to increase product yields from catalytic reactions involve improvement of the properties of the catalytic material or optimization of the catalytic process. To achieve the former, the catalyst activity and selectivity must be enhanced. A bottom-up approach towards the construction of polymer catalysts provides a facile and direct strategy for heterogenization of molecular catalysts. In this way, porous organic polymers (POPs), such as covalent organic frameworks,[1] conjugated microporous polymers,[2] and polymers of intrinsic microporosity,[3] have been exploited for catalysis. Compared with conventional resin-supported catalysts that are often plagued by tedious post-modification and a low loading efficiency,[4] POPs are promising in heterogeneous catalysis[5] because of their high catalyst loading, large surface area, and outstanding catalytic efficiency. Also, the bottom-up approach facilitates the modulation of POPs with tailored porous structure and surface chemistry, and provides an opportunity for the design of polymer frameworks with various functionalities for use as catalysts or ligands.

Diffusion, which is the main mechanism of mass transfer in porous materials, is of pivotal importance for catalysis efficiency, because molecular mobility ultimately determines the rate of the overall process. Active sites within POPs are, however, confined in microporous channels and accordingly impose severe mass-transfer constraints on the rate of catalytic reactions because of the similarity between the size of the involved molecules and the micropore diameter (< 2 nm). Diffusion limitations, which are induced by restricted access and slow transport to/from the active sites, provoke low catalyst utilization over the POPs so that they cannot operate at their full potential. Intensification of the catalytic process for POPs is urgently required, but synthetic challenges remain in the creation of macropores within the microporous frameworks.

Conjugated microporous polymers (CMPs) with stable microporosity and extended conjugated frameworks are one of the most frequently used POPs for heterogeneous catalysis. Such a polymer network could be generated by polymerizing molecular catalysts through conjugated linkers, and provides a high density and accessibility of catalytic centers in a highly stable structure. Depending on the catalytic applications, a variety of catalytic molecules such as metalloporphyrin,[6] binol-derived phosphoric acid,[7] Tröger's base,[8] and N-heterocyclic carbene[9] have been incorporated on CMP skeletons for efficient heterogeneous catalysis. Unlike other POP materials, versatile forms that include colloids,[10] fibers,[11] films,[12] and gels[13] have been explored by adopting different synthetic strategies to promote their functionality and applicability. In this context, we were motivated to incorporate microporous structural inserts into macroporous solids to add another dimension to CMPs. Of the various supports, foams have several appealing features on account of their large geometric areas, high void fractions, high mechanical stability, and low pressure drop. From a technical point of view, CMP solid adsorption on the surface of foams or within voids is feasible, but the loading efficiency is lower than expected. Therefore, a bottom-up synthetic pathway is the more rational option for CMP immobilization within the foam for process-intensified catalysis.

We commenced our study by polymerizing the Zn^{II} complex of 5,10,15,20-tetra(4-ethynylphenyl)porphyrin (ZnTEPP) in the presence of melamine foam through the oxidative homocoupling of terminal alkynes with Pd^{II}/Cu^{I} catalysts in air at room temperature (Figure 1 a). Monolithic melamine foam was submerged in a THF solution of the reactants. Upon addition of the catalysts ($[PdCl_2(PPh_3)_2]$, CuI, and Et_3N), gelation occurred rapidly in an open vial and the monolithic foam was firmly coated and interpenetrated by the ZnP-based CMP gels (ZnP = Zn^{II}-porphyrin). After the reaction, THF in the organogel was exchanged with acetone, which could induce rapid covering of the foam skeletons by CMP and retention of the open cells (about 100 μm). While

[*] K. Y. Wu, Prof. J. Guo, Prof. C. C. Wang
State Key Laboratory of Molecular Engineering of Polymers
Department of Macromolecular Science, Fudan University
No. 220, Handan Road, Shanghai 200433 (China)
E-mail: guojia@fudan.edu.cn

Supporting information for this article can be found under: http://dx.doi.org/10.1002/anie.201600891.

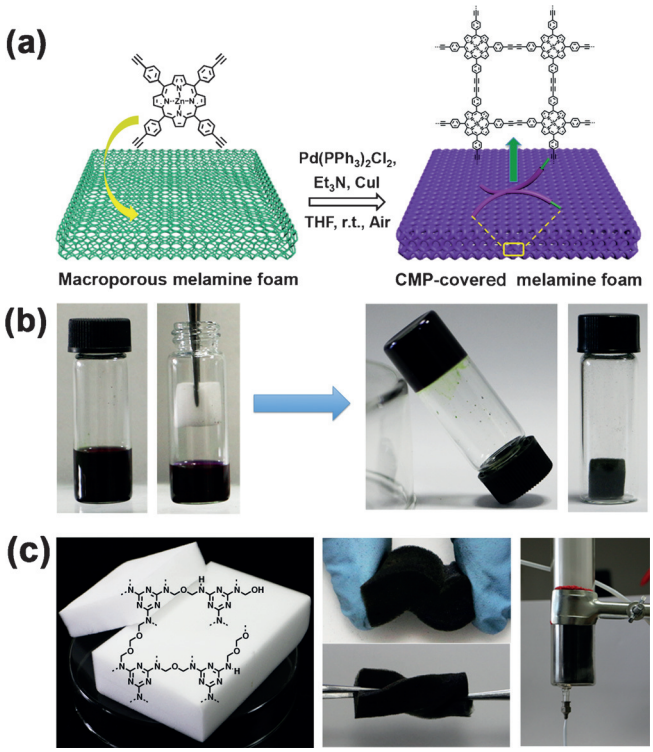

Figure 1. a) The CMP-gel-mediated composite strategy for the preparation of the CMP-covered foam composite. b) The synthetic procedure included: i) mixing of the foam and reaction solution, ii) gelation, and iii) solvent removal and adhesion of CMPs to the foam. c) Photographs of the melamine foam (left) and as-synthesized CMP foam composites (center, right) that could be compressed and distorted and that fill into the glass syringe.

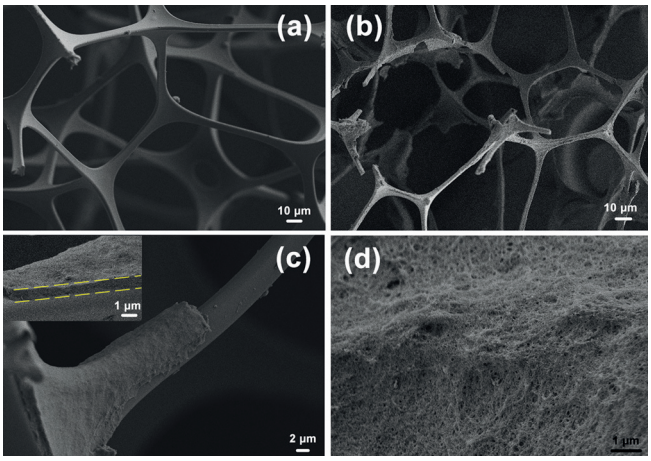

Figure 2. FE SEM images of a) the melamine foam and b–d) the CMP-covered foam composites. Inset in (c): expanded view of the surface of the composite skeletons for estimation of the thickness of the CMP coating. Scale bars in (a, b) = 10 μm; (c) = 2 μm; (d) = 1 μm.

drying under reduced pressure, the white melamine foam turned dark purple and contracted slightly (Figure 1 b). To our knowledge, because of the high rigidity and restricted rotation of repeating units within CMP networks, it has not, to date, been possible to achieve many potential applications of CMPs. However, because a melamine foam support was used in the results reported herein, the ZnP-based frameworks could be subjected to compression and distortion, could fill the column with the form of the foam composite (Figure 1 c), and displayed elastomer characteristics.

Field-emission (FE) SEM images revealed that the smooth melamine framework (Figure 2 a) was encased by the polymerized metalloporphyrin products, which resulted in a surface roughness as shown in Figure 2 b. Some overlaid the foam framework branches with a thickness of 1–2 μm (Figure 2 c and inset), and the other with planar shape was attached to the walls but did not fill the cells. The CMP coatings had a fine-grained aggregate morphology (Figure 2 d). The attempt to cover open-cell foams with CMP was successful by the in situ loading strategy. CMP structures at a molecular level were characterized by solid-state ^{13}C cross-polarization magic angle spinning (CP/MAS) NMR (see Figure S1 in the Supporting Information). The spectra of the xerogels extracted from the foam composites showed signals at $\delta = 120.2$, 130.9, 143.0 and 149.3 ppm, which could be assigned to $C_{pyrrole}$, $C_{ar\text{-}H}$, $C_{ar\text{-}C}$, and C_{ar}-$C_{porphyrin}$ sites, respectively. A resonance signal for the terminal alkyne group on the Zn(TEPP) monomer was not detected, which indicates that the resulting network has a high polymerization degree in the oxidative homocoupling reaction, even though melamine foam was mixed in the reaction. Also, this result implies that the reactant diffusion is rather free in an open-cell foam. Thermogravimetric analysis revealed that the CMP formed in the composite was thermally stable below 500 °C in air (Figure S2). In contrast to the bare foam and CMP powders, the loading content of the CMP coverings reached as high as 53.4 %, and the Zn content was approximately 4.47 %, which was close to the theoretical value (4.81 %). For comparison, we carried out a direct mixing of the CMP powders and melamine foam in THF. Although an excess amount of sample was added, a loading of only 6.8 % was achieved, and the CMP powders were mainly embedded in the hollow cavity from which they could leak after repeated use (Figure S3). This again indicates the superiority of the bottom-up synthetic strategy.

Using the CMP gelation strategy, a wide range of reaction conditions was tested for the construction of CMP coatings around the foam framework. The proportion of CMP to foam was tuned to balance the micro- and macroporous structures by varying the monomer concentrations (Table 1). As the feed amount of Zn(TEPP) was increased from 7.5 to 20 mM under otherwise identical conditions, the composite surface area was enhanced accordingly, and the maximum surface area and pore volume were up to 684 $m^2 g^{-1}$ and 0.23 $cm^3 g^{-1}$, respectively, for composite-3. This trend of increased surface area and pore volume was as a result of increased CMP coatings on the foam framework. As shown in Figure 3 a, nitrogen adsorption–desorption isotherms for the three composites proved that all three have typical microporous character. However, hysteresis at a low relative pressure occurred for composite-1. This often results from a remarkable swelling of the adsorbent upon gas uptake, which implies that the low-density network may deform as increasing numbers of nitrogen molecules condense inside the pores.[14]

Table 1: Porosity parameters of CMP foam composites.

Sample	Zn(TEPP) [mM]	S_{BET}[a] [$m^2 g^{-1}$]	S_{micro}[b] [$m^2 g^{-1}$]	S_{ext}[b] [$m^2 g^{-1}$]	V_{tot}[c] [$cm^3 g^{-1}$]
Melamine Foam	N.A.	15.8	–	–	–
Composite-1	7.5	202.2	156.4	45.8	0.1209
Composite-2	15	587.1	442.0	145.1	0.1921
Composite-3	20	684.1	525.1	159.0	0.2310

[a] Surface area (S_{BET}) is calculated from the N_2 adsorption isotherm using the BET method. [b] The external (S_{ext}) and micropore (S_{micro}) surface areas are obtained using the *t*-plot method based on the Halsey thickness equation. [c] Total pore volume at $P/P_0 = 0.99$.

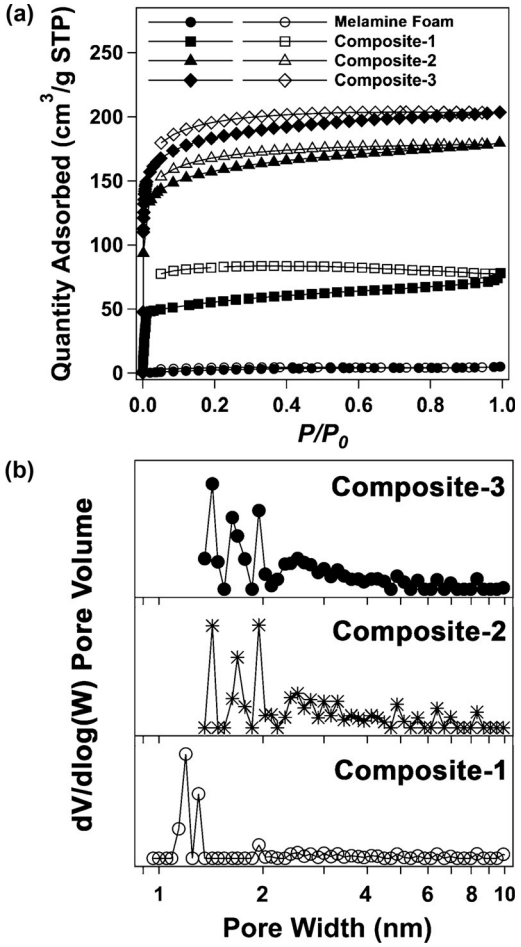

Figure 3. a) Nitrogen adsorption–desorption isotherms of composite-1, composite-2, composite-3, and melamine foam and b) pore size distributions of composites-1–3. In (a), adsorption data points are denoted by filled symbols, whereas desorption data points are denoted by empty symbols.

Pore size distributions were calculated using a nonlocal density functional theory model, and predominant populations ranged from 1 to 3 nm for all composites (Figure 3b). The bare melamine foam did not show any nanoporosity in the nitrogen sorption measurements. After the monomer concentration had been continuously increased, the resultant composite became much harder and smaller. Cells in the foam were filled with CMP products, which lead to a loss of partial macroporosity (Figure S4).

The density of the CMP-covered foam, as determined by accurate measurement of the volume and the mass of composites, was as low as 0.035 $g\,cm^{-3}$ (Figure S5). Compared with the density of the melamine foam (0.011 $g\,cm^{-3}$), the amount of CMP loaded by the gelation-mediated pathway was estimated to be up to 12%, 37%, and 48% for composite-1, composite-2, and composite-3, respectively. The uniformity in texture was proven by examining the densities of small patches cut from the large composite foam (Figure S6). A quantitative analysis of elasticity was carried out to obtain insight into the effect of a CMP covering on the foam body properties. The melamine foam with open cells had a hardness of 6 Shore C (Shore C: indentation hardness with level C) and a resilience value as high as 64%. Upon formation of a CMP layer on the foam framework, the hardness increased slightly to 13 Shore C and its resilience was decreased to 52%. This slight change demonstrates a significant advantage of this system, in that the open-cell melamine foam framework is retained, and suggests that the CMP foam composite could be used for process-intensified catalysis.

Besides its elastic properties, the stability of the composite with repetitive use and exposure to solvents was evaluated. For composite-3, only approximately 2% of the CMP was lost from the support after 50 compression and rebound cycles (Figure S7). We propose that the coordination of the unsaturated ZnP sites to melamine units helps anchor the CMP on the branches of the foam frameworks. We investigated the attachment stability of CMP by immersing the composites in different solvents including water, DMF, DMSO, dioxane, THF, acetone, and chloroform (Figure S8). After one week, all solvents remained colorless and the composite foams were intact without any significant damage.

To demonstrate the catalytic capability of the CMP foam composites, we used the acyl transfer reaction between *N*-acetylimidazole (NAI) and 3-pyridylcarbinol (3-PC). As shown in Figure 4a, product yields on the CMP foam composite-3 were evaluated against the control reactions by applying the CMP powders ($S_{BET} = 874\ m^2 g^{-1}$),[13] Zn(TEPP) monomer, melamine foam, and composite-1 as reference catalysts. The melamine foam exhibited no catalytic activity, which is indicative of its chemical inertness in the reaction. In contrast, the CMP-containing catalysts, that is, the CMP powder, composite-1, and composite-3, accelerated the reaction rate significantly, and were about 2–5 times more active than the Zn(TEPP) monomer. The highest yield was achieved with composite-3 instead of with the CMP powder, although the latter has a higher surface area than composite-3. These results demonstrate that the microporous structures and macroporous channels are both critical to enhance the reaction rate. The repeated use of composite-3 in five runs did not impair the catalytic efficiency (Figure 4b). To our knowledge, the acyl transfer reaction proceeds through a doubly bound intermediate at the host and has been proven to accelerate with a cyclic metalloporphyrin trimer.[15] As shown in Figure 4c, a transition coordination of NAI and 3-PC to the proximal two ZnP sites can stabilize the acyl oxygen in the transition state. Thus, it appears that the Zn(TEPP) monomer provides a small degree of catalytic activity, but the CMP-containing catalysts lead to additional

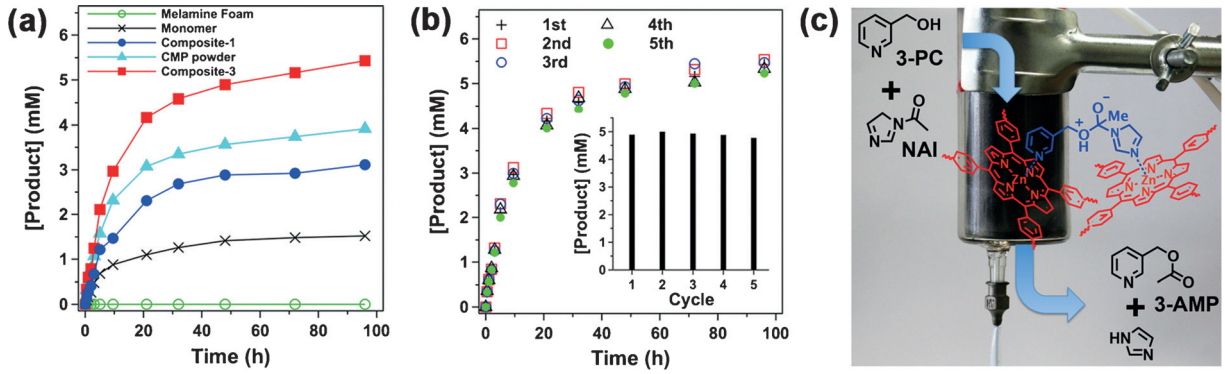

Figure 4. a) Product concentration versus time plots for the formation of 3-(acetoxymethyl)pyridine (3-AMP) from NAI and 3-PC by using the composite-3, composite-1, CMP powder, Zn(TEPP) monomer, and melamine foam as catalysts, respectively. b) Reusability of the CMP foam composite-3 in five reaction runs. c) Representation of the acyl transfer reaction with a doubly bound intermediate in the micropore of ZnP-based frameworks.

acceleration owing to the simultaneous binding of two substrates within the micropores. Regardless of whether the powder or composite form is used, the high-surface-area CMPs could concentrate the reactants in the micropore and increase the reaction rate without changing the activation energy, thereby resulting in an improved catalytic efficiency. However, in the presence of excess substrates, their diffusion in microporous tunnels is inhibited within the fine CMP powders. The open-cell CMP foam composite overcomes this drawback, facilitates the mass transfer, intensifies the catalytic process, and achieves the highest catalytic efficiency.

In summary, our findings introduce an efficient composite strategy that is based on the CMP gelation reaction for the in situ covering of a melamine foam by ZnP-based frameworks. The CMP-gel-mediated method allowed for modulation of the extent of the coating without filling the open cells of the foams. This bottom-up synthetic route is flexible and is widely applicable to other CMP monomers and different supporting substrates for CMP-based composites with a variety of potential end-use applications. By following the route reported herein, a combination of micropores and macropores in the CMP-covered foam composite was created for the first time. The unique structure of the material has exceptional stability, functions as an elastomer, and can intensify the catalysis process. The specialized design of the composite fulfils industrial directives and may provide an access route to more efficiently supported catalysts for specific reactions.

Acknowledgements

This work is supported by the NSFC (21474015) and STCSM (14ZR1402300).

Keywords: conjugated polymers · foam composites · gels · porosity · supported catalysts

How to cite: *Angew. Chem. Int. Ed.* **2016**, *55*, 6013–6017
Angew. Chem. **2016**, *128*, 6117–6121

[1] a) A. P. Côté, A. I. Benin, N. W. Ockwig, M. O'Keeffe, A. J. Matzger, O. M. Yaghi, *Science* **2005**, *310*, 1166–1170; b) J. W. Colson, A. R. Woll, A. Mukherjee, M. P. Levendorf, E. L. Spitler, V. B. Shields, M. G. Spencer, J. Park, W. R. Dichtel, *Science* **2011**, *332*, 228–231; c) X. Feng, X. Ding, D. Jiang, *Chem. Soc. Rev.* **2012**, *41*, 6010–6022; d) P. J. Waller, F. Gándara, O. M. Yaghi, *Acc. Chem. Res.* **2015**, *48*, 3053–3063; e) S. Lin, C. S. Diercks, Y.-B. Zhang, N. Kornienko, E. M. Nichols, Y. Zhao, A. R. Paris, D. Kim, P. Yang, O. M. Yaghi, C. J. Chang, *Science* **2015**, *349*, 1208–1213.

[2] a) J.-X. Jiang, F. Su, A. Trewin, C. D. Wood, N. L. Campbell, H. Niu, C. Dickinson, A. Y. Ganin, M. J. Rosseinsky, Y. Z. Khimyak, A. I. Cooper, *Angew. Chem. Int. Ed.* **2007**, *46*, 8574–8578; *Angew. Chem.* **2007**, *119*, 8728–8732; b) A. I. Cooper, *Adv. Mater.* **2009**, *21*, 1291–1295; c) Y. Xu, S. Jin, H. Xu, A. Nagai, D. Jiang, *Chem. Soc. Rev.* **2013**, *42*, 8012–8031.

[3] N. B. McKeown, P. M. Budd, *Chem. Soc. Rev.* **2006**, *35*, 675–683.

[4] a) M. Gruttadauria, F. Giacalone, R. Noto, *Chem. Soc. Rev.* **2008**, *37*, 1666–1688; b) S. H. Youk, S. H. Oh, H. S. Rho, J. E. Lee, J. W. Lee, C. E. Song, *Chem. Commun.* **2009**, 2220–2222; c) M. Heitbaum, F. Glorius, I. Escher, *Angew. Chem. Int. Ed.* **2006**, *45*, 4732–4762; *Angew. Chem.* **2006**, *118*, 4850–4881.

[5] a) Y. Zhang, S. N. Riduan, *Chem. Soc. Rev.* **2012**, *41*, 2083–2094; b) P. Kaur, J. T. Hupp, S. T. Nguyen, *ACS Catal.* **2011**, *1*, 819–835.

[6] a) L. Chen, Y. Yang, D. Jiang, *J. Am. Chem. Soc.* **2010**, *132*, 9138–9143; b) L. Chen, Y. Yang, Z. Guo, D. Jiang, *Adv. Mater.* **2011**, *23*, 3149–3154; c) R. K. Totten, Y.-S. Kim, M. H. Weston, O. K. Farha, J. T. Hupp, S. T. Nguyen, *J. Am. Chem. Soc.* **2013**, *135*, 11720–11723; d) Z. Xiang, Y. Xue, D. Cao, L. Huang, J.-F. Chen, L. Dai, *Angew. Chem. Int. Ed.* **2014**, *53*, 2433–2437; *Angew. Chem.* **2014**, *126*, 2465–2469.

[7] D. S. Kundu, J. Schmidt, C. Bleschke, A. Thomas, S. Blechert, *Angew. Chem. Int. Ed.* **2012**, *51*, 5456–5459; *Angew. Chem.* **2012**, *124*, 5552–5555.

[8] a) X. Du, Y. Sun, B. Tan, Q. Teng, X. Yao, C. Su, W. Wang, *Chem. Commun.* **2010**, *46*, 970–972; b) Z.-Z. Yang, H. Zhang, B. Yu, Y. Zhao, G. Ji, Z. Liu, *Chem. Commun.* **2015**, *51*, 1271–1274.

[9] M. Rose, A. Notzon, M. Heitbaum, G. Nickerl, S. Paasch, E. Brunner, F. Glorius, S. Kaskel, *Chem. Commun.* **2011**, *47*, 4814–4816.

[10] a) P. Zhang, Z. Weng, J. Guo, C. Wang, *Chem. Mater.* **2011**, *23*, 5243–5249; b) K. Wu, J. Guo, C. Wang, *Chem. Commun.* **2014**, *50*, 695–697; c) P. Zhang, K. Wu, J. Guo, C. Wang, *ACS Macro Lett.* **2014**, *3*, 1139–1144; d) J. Tan, J. Wan, J. Guo, C. Wang, *Chem. Commun.* **2015**, *51*, 17394–17397; e) N. Kang, J. H. Park,

M. Jin, N. Park, S. M. Lee, H. J. Kim, J. M. Kim, S. U. Son, *J. Am. Chem. Soc.* **2013**, *135*, 19115 – 19118.
[11] a) X. Feng, Y. Liang, L. Zhi, A. Thomas, D. Wu, I. Lieberwirth, U. Kolb, K. Müllen, *Adv. Funct. Mater.* **2009**, *19*, 2125 – 2129; b) N. Kang, J. H. Park, J. Choi, J. Jin, J. Chun, I. G. Jung, J. Jeong, J.-G. Park, S. M. Lee, H. J. Kim, S. U. Son, *Angew. Chem. Int. Ed.* **2012**, *51*, 6626 – 6630; *Angew. Chem.* **2012**, *124*, 6730 – 6734; c) Y. Chen, H. Sun, R. Yang, T. Wang, C. Pei, Z. Xiang, Z. Zhu, W. Liang, A. Li, W. Deng, *J. Mater. Chem. A* **2015**, *3*, 87 – 91.
[12] a) C. Gu, Y. Chen, Z. Zhang, S. Xue, S. Sun, K. Zhang, C. Zhong, H. Zhang, Y. Pan, Y. Lv, Y. Yang, F. Li, S. Zhang, F. Huang, Y. Ma, *Adv. Mater.* **2013**, *25*, 3443 – 3448; b) C. Gu, N. Huang, J. Gao, F. Xu, Y. Xu, D. Jiang, *Angew. Chem. Int. Ed.* **2014**, *53*, 4850 – 4855; *Angew. Chem.* **2014**, *126*, 4950 – 4955; c) C. Gu, N. Huang, Y. Chen, L. Qin, H. Xu, S. Zhang, F. Li, Y. Ma, D. Jiang, *Angew. Chem. Int. Ed.* **2015**, *54*, 13594 – 13598; *Angew. Chem.* **2015**, *127*, 13798 – 13802.
[13] K. Wu, J. Guo, C. Wang, *Chem. Mater.* **2014**, *26*, 6241 – 6250.
[14] a) J. Weber, A. Thomas, *J. Am. Chem. Soc.* **2008**, *130*, 6334 – 6335; b) J. Schmidt, J. Weber, J. D. Epping, M. Antonietti, A. Thomas, *Adv. Mater.* **2009**, *21*, 702 – 705.
[15] a) L. G. Mackay, R. S. Wylie, J. K. M. Sanders, *J. Am. Chem. Soc.* **1994**, *116*, 3141 – 3142; b) C. G. Oliveri, N. C. Gianneschi, S. T. Nguyen, C. A. Mirkin, C. L. Stern, Z. Wawrzak, M. Pink, *J. Am. Chem. Soc.* **2006**, *128*, 16286 – 16296.

Received: January 26, 2016
Published online: April 8, 2016

